*17th World Conference on Earthquake Engineering, 17WCEE*

*Sendai, Japan - September 13th to 18th 2020*

# Study on practical performance of reasonably-priced acceleration sensors based on shaking table tests and strong motion observations.

K. Nakano[1], H. Kosaka[2], T. Yamamoto[3], and T. Kashima[4]

[1] *Researcher, HAZAMA ANDO CORPORATION, nakano.kenichi@ad-hzm.co.jp*
[2] *Researcher, TODA CORPORATION, hiroyuki.kosaka@toda.co.jp*
[3] *Researcher, TODA CORPORATION, takeshi.yamamoto2@toda.co.jp*
[4] *Researcher, Building Research Institute, kashima@kenken.go.jp*

## *Abstract*

Many inexpensive measuring devices equipped with MEMS sensors have been developed. For example, smart devices (or smartphones) have a 3-axis accelerometer and a network module (i.e. LTE/3G), therefore we will be able to conduct the strong motion observations using these devices, quite easily. On the other hand, there have been few studies about the performance of those as the seismometers yet. But we should confirm whether the devices are suitable for our objectives, because the detailed information about the sensor with smart devices as seismometers (i.e., sensitivity or measurable range of devices) are unclear in many cases. Therefore, in this research, we performed the shaking table test to evaluate the measurement performance of the devices as seismometers. At first, we selected the seven types of seismometers with MEMS sensors (including smartphones), which are cheaper than approximately $1,000 per unit in Japan. We also adopted the servo-type accelerographs (JU410) for comparison. The table (6m long by 4m wide) were shaken by 3-axis input waveforms. We used the waves observed at Kobe marine observatory in the 1995 Hyogo-ken nanbu earthquake, for the shaking table test. Through shaking table test, we found that some of the measurement devices have almost the same performance as the servo-type accelerographs up to 0.2-20 Hz, comparing Fourier spectral ratios based on servo-type accelerographs. We also found that the performance of devices correlated positively with the price of devices. To evaluate the performance of devices for the strong motions with several tens of cm/s$^2$ (ground motions with this level of amplitude frequently occurs a day anywhere in Japan), we performed strong motion observations using the five devices equipped with MEMS sensor in a six-story wooden building from Jul. 5, 2018.The strong motion observation with servo-type accelerometers (CV374) have been operated in the same building. At 20:23, Jul. 7, 2018, an earthquake with $M_{\mathrm{JMA}}$ 6.0 at offshore Chiba prefecture occurred, and the ground motions were recorded at these instruments. The right panel of Figure 1 shows the comparison of spectral ratios with MEMS sensors based on CV374. We found that the Fourier spectral ratios (amplitude) of sensor “F” and “S” in approximately 0.3 to 5 Hz are substantially matched well with CV374, and, the Fourier spectral ratios (phase) in approximately 0.2 to 10 Hz are also matched well.

*Keywords: MEMS, Smart device, Strong motion observation*

## 1. Introduction

There have been many attempts to use vibration measurements from microtremors and ground motion to evaluate the soundness of structures damaged by an earthquake for example [1][2]. A system of evaluation techniques is typically called health monitoring [3] and is not limited to the field of architecture. The system specializing in structure fitness evaluation is especially known as structural health monitoring (SHM). Its effectiveness is attracting renewed attention after the earthquake off the Pacific coast of Tohoku in 2011 [4], and SHM is now becoming widely recognized.

Real-time estimation after a disaster is required in SHM, thus SHM is generally incorporated as a system that automatically evaluates the soundness of a building for example [5]. Real-time estimation without failure after a disaster is demanded in such a system, thus redundancy in the entire network consisting of seismometers and recording devices, as well as stability of the system (including obtaining high precision vibration records, time synchronization between sensors, and data collection), must be guaranteed. As a consequence, systems often use expensive sensors such as servo-type accelerometers.

Strong motion observation is a field that has many differences but is often confused with SHM. Both have similarities on the hardware side, where the system measures the oscillation of a structure using sensors, and on the software side, where the measured vibration is evaluated by signal processing technology. However, the objectives of SHM and strong motion observation are different; the former evaluates the soundness of the target structure in real time but the latter aims to obtain insights obtained by, for example, verification of design in the target structure and provide feedback toward the next design. This difference clearly distinguishes the two concepts, but there is much common ground in both hardware and software aspects, and therefore they appear similar to the general public [6]. There are two targets of strong motion observation, which are the soil and building systems. Examples of strong motion observation networks in Japan are K-NET [7] and KiK-net [8] of the National Research Institute for Earth Science and Disaster Resilience (NIED) for the soil system, and the BRI Strong Motion Network of the Building Research Institute (BRI) for the building system. The measurement points are scattered all over Japan, and the observed strong motion waveforms are utilized not just in the seismic design of the structures but also in various applications including understanding of the physical phenomena in seismology and earthquake engineering. Therefore, strong motion observation could be regarded as infrastructure in the vibration engineering field [6]. Micro electro mechanical systems (MEMS) sensors are becoming smaller, more sophisticated, and less expensive in recent years. This is fueled by the rapid global move toward the Internet of things (IoT). The dissemination of smartphones is especially remarkable [9]. Smartphones contain all the functions necessary as a seismometer (acceleration sensor, recording device, and time synchronization through a network time protocol (NTP) server), and there are reports of earthquake observations using smartphones [10]. There are efforts to treat measured vibration data loaded on cloud storage as big data and utilize it in disaster prevention [11]. However, measurement devices containing MEMS sensors are currently not widely used as seismometers, and the vibration measurement performance is not well understood. Therefore, confirming that measurement devices containing low-cost MEMS sensors have sufficient vibration measurement performance for strong motion observation or SHM is beneficial.

The goal of this research is to utilize measurement devices loaded with inexpensive MEMS sensors as seismometers, after evaluating the performance of those. First, vibration measurement performance evaluation tests were conducted using a large triaxial shaking table and a full-scale vibration test system. The measurement devices were then installed on a six-story wooden test building [12]. Strong motion observations were conducted to confirm the measurement performance of real seismic motion, and the performance of each measurement device as a seismometer for strong motion observation was verified. This paper discusses buildings among structures.



 

## 2. Meaning of using MEMS sensors as measurement devices

This section discusses the meaning of using measurement devices containing MEMS sensors as seismometers and clarifies the positioning of this research. The history of strong motion observation in Japan is reviewed, the current status of SHM is outlined, and the outlook of using MEMS sensors in SHM is discussed.

There is a long history of strong motion observation in Japan, which is said to have started on July 29, 1953 when a Strong Motion Accelerometer Committee (SMAC)-type accelerometer was installed in the Earthquake Research Institute, University of Tokyo [13]. SMAC-type accelerometers were installed mostly in buildings because these were developed after damage from the 1948 Fukui Earthquake. The ultimate aim of SMAC-type accelerometers was to provide feedback on seismic design, according to Takahashi [14]. This is the reason for the objective of strong motion observation as mentioned above, which is "to obtain insights obtained by, for example, verification of design in the target structure and provide feedback toward the next design". The advent of SMAC-type accelerometers led to recording of strong motion waveforms, such as from the 1964 Niigata Earthquake and the 1968 Tokachi-oki Earthquake, over a wide region. The Meteorological Agency developed the 87-type electromagnetic accelerometers to promote wide area and wide frequency range strong motion observation in Japan. These accelerometers were replaced with the 95-type after 1995. Following the 1995 Hyogo-ken Nanbu earthquake, NIED started operation of the ground surface strong-motion seismograph network K-NET [7] and KiK-net [8].

The BRI started preparing a strong motion observation network since 1957 using SMAC-type accelerometers mentioned earlier. Observations continue today, and measurement equipment is being updated [15]. The BRI network is the only building-system strong motion observation network where data is made public and all of Japan is covered. This is a result of complicated circumstances. For example, strong motion observation data of a building belongs to the owner of the building, and observation data includes important information on design and construction.

The current strong motion observation aim is to "not miss the strong motion waveform (vibration response waveform)" and "understand vibration and seismic phenomena and provide feedback on seismic design", thus servo-type accelerometers that are stable and have recording accuracy with high quality are used as measurement devices (sensors). However, servo-type accelerometers are generally expensive (more than half a million to a few million yen), and installing multiple sensors in a high-rise office building can result in a total expense of around 10 million yen. Therefore, strong motion observation is not conducted in many private buildings because of the cost performance with regards to the initial investment. Strong motion waveforms have not been recorded for the 2016 Kumamoto Earthquake in base isolated buildings (within the scope of openly available data) [16]. This fact implies that a sufficient building-system strong motion network is not available as infrastructure. On the other hand, even without servo-type accelerometer seismometers, installment of seismometers with low-cost MEMS sensors could have provided very precious insights on the seismic design of buildings. Therefore, actively installing affordable MEMS sensors for strong motion observation has very significant meaning.

SHM is gaining attraction after the aforementioned 2011 off the Pacific coast of Tohoku Earthquake. Measures by Tokyo Metropolis regarding stranded commuters, which were designated after this earthquake, mandated that building owners judge whether a building could be continued to be used within about three hours of an earthquake [17]. As such, businesses owning buildings over a certain size are starting to install SHM systems. Now, there are ongoing studies to grasp the damage a building may incur in detail. In an E-defense experiment, an SHM system was built that evaluates the disaster situation in detail and the cumulative damage by installing about 150 MEMS acceleration sensors, mostly at pillar-beam joints, on a 1/3 scale 18-story steel frame building [18]. This is in a test stage, but low-cost sensors are definitely necessary because many sensors are installed on a building. There also demands for coarse information, which is in contrast to aforementioned requests for understanding the details of the damage situation. For example, some building owners may only need to know the seismic intensity of the first or highest story. Therefore, the use of servo-type accelerometers is not necessarily the optimum solution for such needs.



 

Therefore, consideration of the use of affordable measurement devices is a very natural trend and can be easily understood.

Table 1 shows our summary of the differences between strong motion observation and SHM (some information is listed in Reference [6]. The objectives of strong motion observation and SHM are totally different, as is evident from this table. Strong motion observation requires both real-time and temporal information, while real-time information is typically sufficient in SHM. The vibration response characteristics of buildings are evaluated by signal processing of data obtained by sensors in both cases, but the importance of feedback is higher in the latter for both building users and owners. The information must be processed into “building soundness”, which is a concept that laymen can digest. Here, primary information obtained using signal processing technologies, such as vibration response and its characteristics, are not necessary.

The situation of current earthquake observation systems is outlined next. There are both distributed and concentrated earthquake observation systems. The sensor and data recording parts are combined in the former while the latter sends data recorded by sensors to the data recording part through signal cables such as BNC cables [19]. Even in the former, sensors are often connected using cables in strong motion observation and SHM to synchronize time and collect data. Possible reasons are conducting soundness evaluation using an on-site computer and ensuring a robust communications environment and time synchronization. Wireless communication using multi-hop technology has been established recently for example [20] and being deployed in SHM. According to Reference [20], communication robustness and time synchronization precision, which have been considered challenges, were resolved at a high standard. This means that the currently adopted cable communications can be replaced by wireless communications. This takes away the need for signal cable pathways and installation, thus installation time and cost can be reduced. Reference [20] achieved a low-cost earthquake observation system by combining wireless communication technologies and MEMS sensors.

The building owner not being prompt in the installation of sensors is an obstacle to the dissemination in both strong motion observation and SHM. Being able to evaluate the soundness immediately after a disaster should be a huge benefit. However, most people think that seismic motion that causes damage to a building does not happen many times during a building’s lifetime, thus building owners do not install sensors quickly, which is one reason that strong motion observation and SHM do not become commonplace. Therefore, a combined monitoring system is proposed where the building equipment is monitored during normal times and SHM is conducted in an emergency (disaster) [21]. Use of MEMS sensors that can be easily combined with various measurement devices and perform data communications would be advantageous in such situations. The acceleration sensor performance specifications necessary to act as a seismometer for strong motion observation was reported in the Third Strong Motion Observation Symposium of the Architectural Institute of Japan in 2002 [22]. Recent MEMS sensors on the market should have sufficient precision. The above discussions indicate that using measurement devices containing inexpensive MEMS sensors is an important approach to deploy strong motion observation and SHM.

Table 1 – Differences in strong motion observation and SHM of buildings.

| Requiring item | | | Strong Motion Observation | Structural Health Monitoring |
|---|---|---|---|---|
| Objectives | State of building | Change in case of disaster | ◎ | ○ |
| | | Ageing | ◎ | △ |
| | Evaluation for damage | | △ | ◎ |
| Priority | End-user | | 4 | 1 |
| | Building owner | | 3 | 2 |
| | Structural designer | | 2 | 3 |
| | Researcher | | 1 | 4 |
| Data analysis | Stand-alone | | ○ | ○ |
| | cloud network | | ◎ | ○ |
| | Application | | △ | ◎ |



 

## 3. Measurement performance evaluation of MEMS sensors

### 3.1 Measurement performance grasp test using shaking table

Tests using a vibration machine were conducted to evaluate the vibration measurement performance of measurement devices containing MEMS sensors. A large triaxial shaking table owned by the author's institution was employed, and the strong motion waveform of the 1995 Hyogo-ken Nanbu earthquake observed at the Kobe Marine Observatory was used. Excitations were applied on the shaking table to reproduce the original wave. Table 2 shows a list of measurement devices tested in this research, and Photo 1 shows how the measurement devices were fixed on the shaking table. Details of the tests are given in reference [23]. The waveform measured by the measurement device (sensor) J-3 was used as the reference waveform, and the measurement performance was compared using the Fourier spectrum ratio based on the cross-spectrum with the waveform from each measurement device (Fig. 1). The measured waveform along the north-south (NS) direction (x-axis in Photo 1) was compared here, and the spectrum ratio was taken after adjusting for the time difference by comparing the phase angle of each waveform against the reference waveform. The sampling rate of the measurement devices was 100 Hz. The terms "measurement device" and "sensor" have the same meaning in the following discussion.

The following can be deduced by comparing the Fourier spectrum amplitude ratios in Fig. 1A: the amplitude ratio for sensor G-1 was roughly in unity to about 10 Hz although there were some differences between individuals on the long period side (about 0.2-0.4 Hz), and there was much scattering as a whole in sensor G-1c, while sensors G-1a and G-1b were relatively stable. The amplitude ratio of sensor G-2 was approximately in unity in the 0.4-2 Hz range but decreased suddenly above 2 Hz. A similar trend was found in other investigations, thus signals from this sensor should have passed a low-pass filter. Similarly, Fig. 1B shows Fourier spectrum ratios for sensors A-1 to A-4. There was less overall scattering compared to Fig. 1A, and the amplitude ratio was roughly in unity over a wide frequency range of 0.2–10 Hz. The amplitude ratio was about in unity, and the scattering was small above 10 Hz in sensors A-1 and A-2, but the characteristics indicate passage through a weak low-pass filter. Fig. 1C and 1D show a comparison of the Fourier spectrum phase ratio. Fig. 1C compares sensors G-1 and G-2, while Fig. 1D compares sensors A-1 to A-4. These results confirm that the scattering of sensors A-1 to A-4 was smaller than sensors G-1 and G2, and the phase delay was zero over a wide frequency range. Most notably, the phase delay of sensors A-1 and A-2 was almost zero over the range 0.2-20 Hz.

Table 2 – Measurement devices used in tests with a shaking table.

| Code | Year | Name | Number |
|---|---|---|---|
| G-1 | 2015 | Geo-stick | 3 |
| G-2 | 2015 | GID-SSS | 1 |
| A-1 | 2017 | ipad pro | 1 |
| A-2 | 2017 | iphone 8 plus | 1 |
| A-3 | 2016 | iphone 7 | 2 |
| A-4 | 2012 | ipod (5th gen.) | 1 |
| J | 2016 | JU410 | 5 |

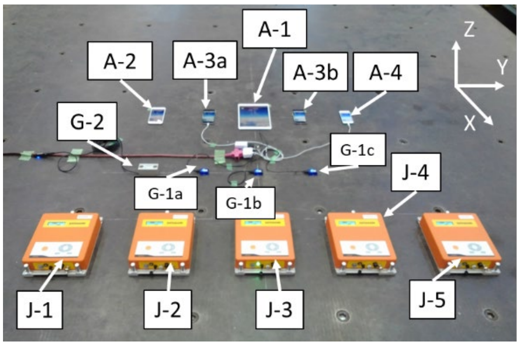


Photo 1 – Positions of measurement devices on the shaking table.

### 3.2 Measurement performance grasp test using full-scale vibration test equipment

To reproduce seismic motion in a more realistic building, we subsequently conducted measurement performance evaluation tests on measurement devices containing MEMS sensors with a full-scale vibration test system owned by the institution to which one of the authors belong.



 

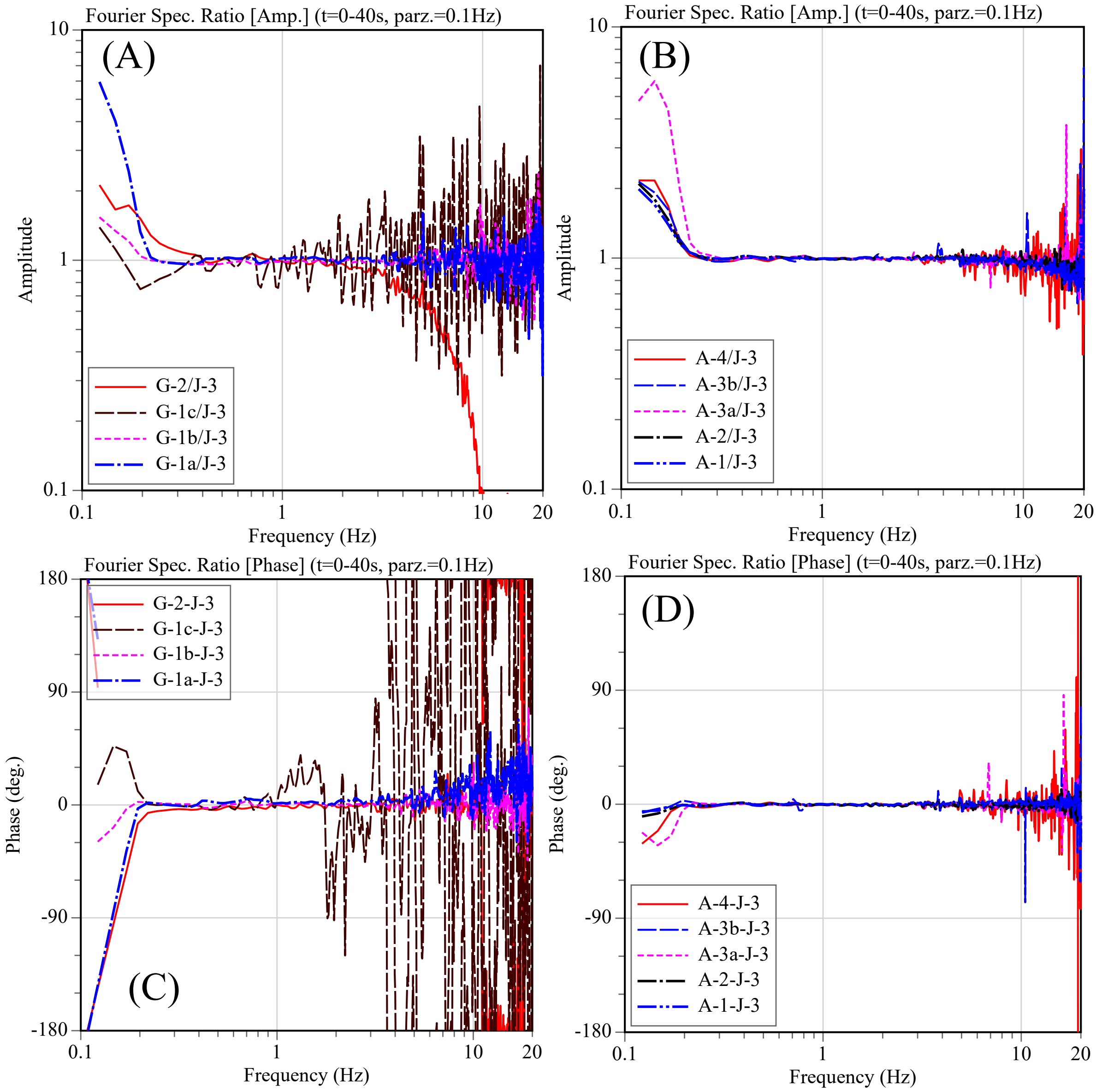


Fig. 1 – Comparison of measurement performance between measurement devices. A: amplitudes of G-1a, G-1b, G-1c, G-2, B: amplitudes of A-1, A-2, A-3a, A-3b, A-4, C: phases of G-1a, G-1b, G-1c, G-2, and D: phases of A-1, A-2, A-3a, A-3b, A-4.

The full-scale vibration test system has a multiple isolation structure and is equipped with seismic isolators at the foundation and on a middle story (Fig. 2). There is an active mass damper (AMD) on the roof. The test system can be vibrated in the horizontal two axes by providing an excitation wave as input to the AMD (see Watabe et al. [24]) for details on this system). Table 3 shows a list of measurement devices tested. The excitation waveform was the strong motion waveform of the 1995 Hyogo-ken Nanbu earthquake used earlier (NS-direction waveform excitations in two directions at the same time), and the amplitude of the excitation waveform was adjusted such that the seismic intensity is about a scale 4 at the measurement story. The waveform from sensor L, which is a servo-type accelerometer, was used as the reference waveform for comparison. The sampling rate and time synchronization methods depend on the specifications of each measurement device. Thus, comparison was conducted after down-sampling to 50 Hz and adjusting time using a cross-correlation function. The maximum measured acceleration was about 30 cm/s$^2$. The tests in this section aimed to investigate the minimum motion that can be detected by MEMS acceleration sensors, thus the intention was measurement of weak motion.

Fig. 3 compares the Y-direction waveform spectrum ratios versus sensor L measured in the full-scale vibration test. Fig. 3A gives the Fourier spectrum amplitude ratios of sensors A-1, A-2, G-1, and G-2 to sensor L; and Fig. 3B shows the ratios of sensors J, X, and F to sensor L. The results show that there was a good agreement between a range of approximately 0.6 to 3 Hz although there was some scattering. The measurement performance seems slightly worse than in the previous section, but this is because the amplitude of the excitation waveform was adjusted such that the seismic intensity is about a scale 4 at the measurement story. In other words, the difference arises from the lowering in apparent signal-to-noise ratio (S/N) of MEMS sensors [25]. Fig. 3C and D compares the Fourier spectrum phase ratios. The overall trend is the same as Fig. 3A and B. Please refer to reference [26] for details on the verification in this section.

Table 3 – List of measurement devices used in the full-scale vibration test.

| Condition | L | A-1 | A-2 | G-1 | G-2 | J | X | F |
|---|---|---|---|---|---|---|---|---|
| Code | LS-10C | - | ipad | Geo stick | GID-SSS | JW24F14 | - | MEMS-Applied Vibration Sensor |
| Type of sensor | Servo | MEMS | MEMS | MEMS | MEMS | MEMS | MEMS | MEMS |
| Samples (Hz) | 200 | 200 | 100 | 100 | 100 | 125 | 200 | 200 |
| Number of Ch. | 2 | 3 | 3 | 3 | 3 | 3 | 3 | 3 |

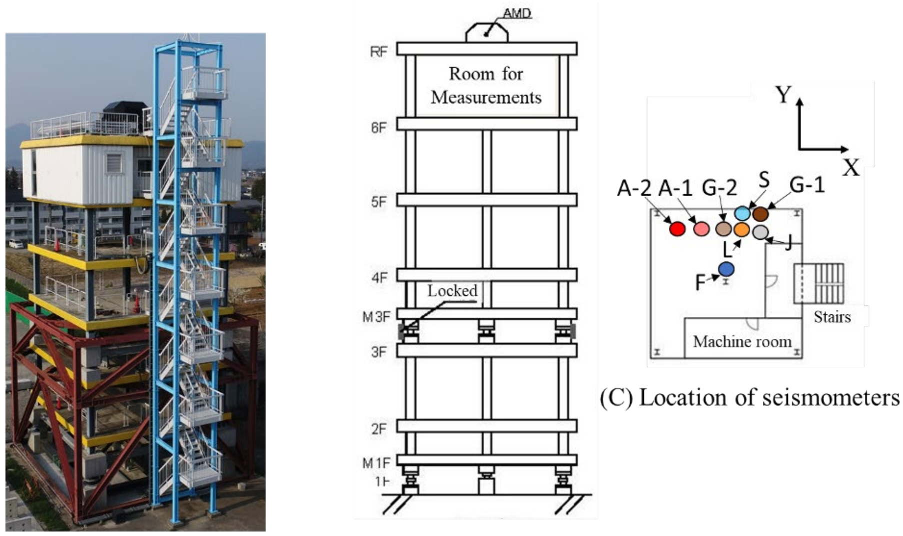


(A) Exterior view of the full-scale test system

(B) Elevation of the full-scale test system

(C) Location of seismometers

Fig. 2 – The full-scale vibration test system and location of seismometers.

## 4. Strong motion observation in a 6-story wooden experimental house using a MEMS sensor

### 4.1 Outline of strong motion observation

The discussion up to the previous section showed that some measurement devices containing MEMS sensors have measurement capabilities comparable to servo type accelerometers for a certain signal strength and frequency range. Our discussion was based on results from ideal measurement environments where signals



 

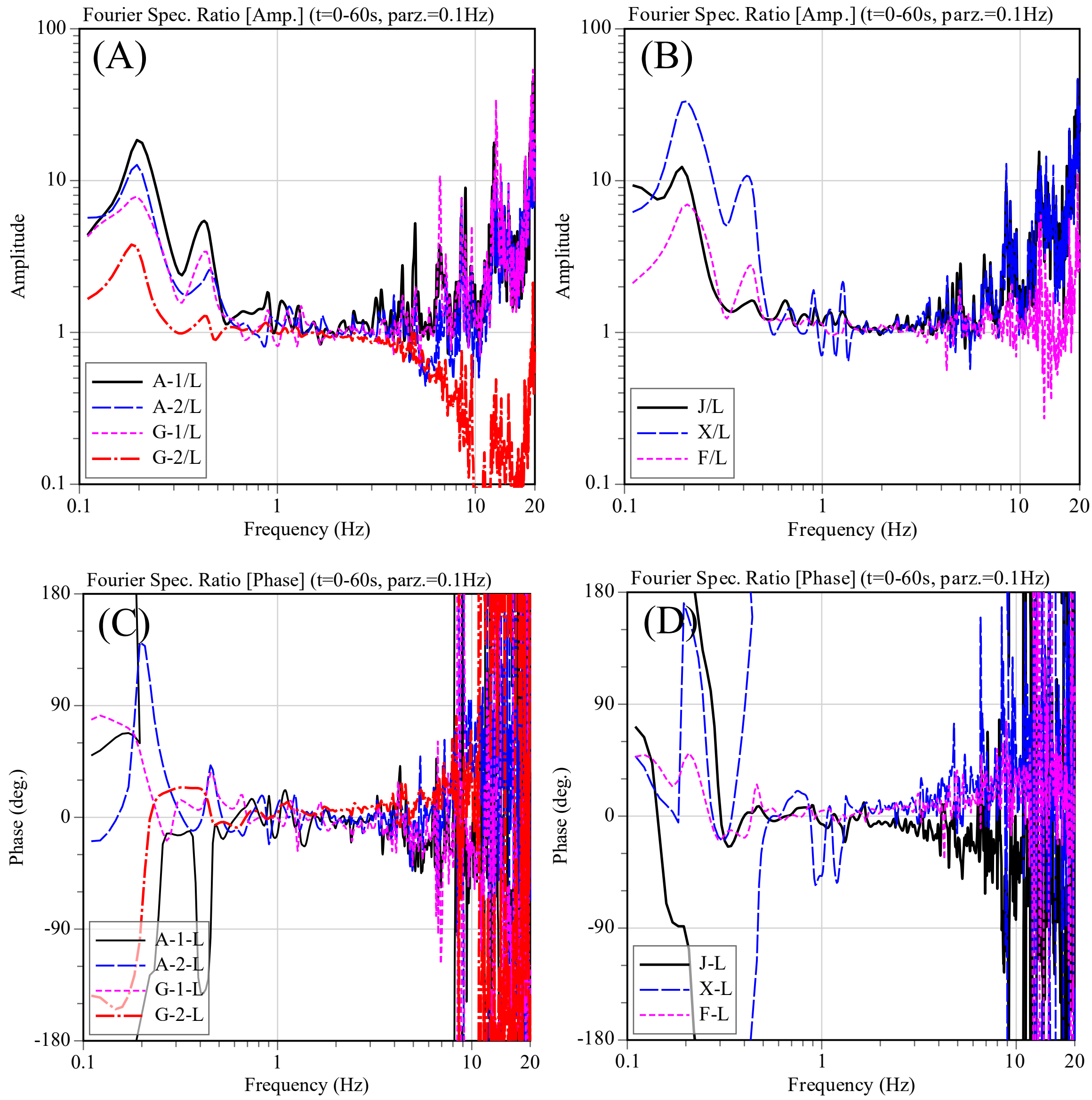


Fig. 3 – Comparison of Fourier spectrum ratios measured with the full-scale vibration test.

were measured after artificially exciting a vibration machine or a full-scale vibration test system using a strong motion waveform. Therefore, the next task is to verify the performance of measurement devices in a measurement environment comparable to real residences.

There is a six-story wooden test building in the premises of the BRI. The objective of this building is to verify and promote technologies to develop high-rise wooding buildings, therefore it was realistically designed and constructed for use as a typical residence as shown in Photo 2. One of the authors has installed seismometers including servo-type accelerometers and is continuing strong motion observations in this building [27].

We installed measurement devices shown in Table 4 to this building, which matches our objectives. Strong motion observations started on July 5, 2018. Fig. 4 shows the locations of measurement devices installed in this research. Sensors C and F are already installed seismometers and synchronize time using GPS signals and a NTP server, respectively. Regarding the newly installed measurement devices, sensors A and S synchronized time with an NTP server, while sensors G-1 and G-2 used the clock in the measurement computer. Sensor S synchronized time and communicated time with each other by wireless communication and not through cables.

## 4.2 Comparison of vibration measurement performance of MEMS sensors

In Many seismic waveforms have been obtained from the ongoing strong motion observation. We compare vibration measurement performance using the NS-direction waveform obtained from an earthquake off the east coast of Chiba prefecture at 8:33 pm, July 7, 2018 ($M_{JMA}$6.0) in this article. Sensor C is used as the reference because this is a servo-type accelerometer. There were differences in the absolute time between MEMS sensors because of the specifications, thus differences in time were adjusted as in Section 3.1. The waveforms observed at the sixth story are obtained here. The maximum acceleration was about 45 cm/s$^2$.

Fig. 5 shows the Fourier spectrum ratios of waveforms observed by measurement devices in Table 3 (the reference is sensor C). Fig. 5A and 5B compare the amplitude and phase, respectively. As it is evident, the amplitude and phases roughly agreed with the servo-type accelerometer in the frequency range of about 0.3-5 Hz and 0.2-10 Hz, respectively. Sensors F and S were very consistent with sensor C, while sensor A shows a similar measurement performance as a whole. Sensors A, F, and S agreed well in the range of 0.3-10 Hz, but the general performances of sensors F and S were better than sensors A. Sensor F was slightly more consistent with sensor C than with sensor S. Note that the comparison of the G-1 sensor was only for the main dynamic part because of triggering issues.

Table 4 – List of measurement devices installed for strong motion observation.

| Condition | C | F | A | S | G-1 | G-2 |
|---|---|---|---|---|---|---|
| Code | CV374 | MEMS-Applied Vibration Sensor | iphone 7 plus | sonas x01 | Geo stick | GID-SSS |
| Type of sensor | Servo | MEMS | MEMS | MEMS | MEMS | MEMS |
| Samples (Hz) | 100 | 100 | 100 | 100 | 100 | 100 |
| Number of sensor | 2 | 8 | 1 | 6 | 3 | 1 |

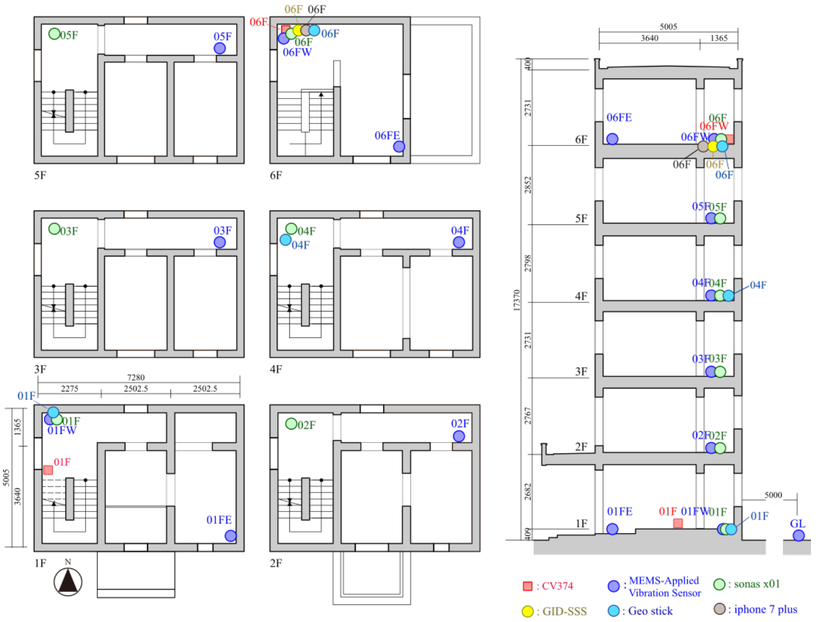


Fig. 4 – Locations of existing seismometers and measurement devices containing MEMS sensors.

Photo 2 – Exterior view of the six-story wooden test building



 

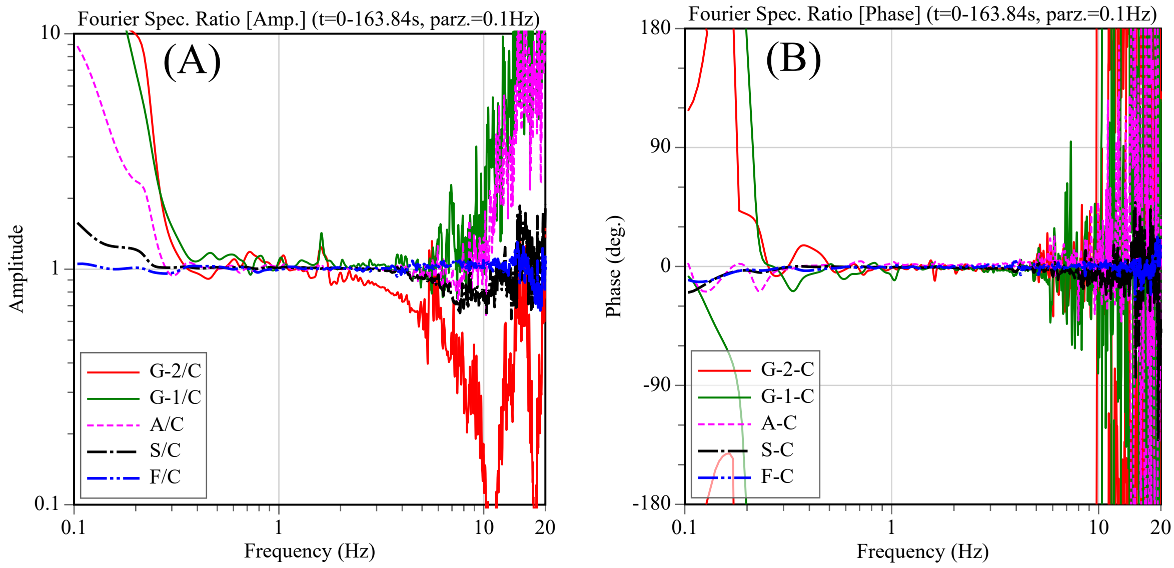


Fig. 5 – Comparison of Fourier spectrum ratios from strong motion observations.

## 5. Conclusion

The summaries from this study are as follows.

- Shaking table tests and full-scale vibration tests showed that, for strong motion waveforms where the amplitude reaches a few hundred cm/s$^2$, some measurement devices containing MEMS sensors give roughly consistent results with servo-type accelerators in the 0.2 - 20 Hz frequency range. On the other hand, a similar consistence was found in the 0.6 - 3 Hz frequency range when the amplitude was a few tens of cm/s$^2$.
- A comparison of the seismic waveforms of measurement devices from ongoing strong motion observation in a six-story wooden test building showed that consistence with a servo-type accelerometer was found for about 0.3-5 Hz and 0.2-10 Hz ranges in the Fourier spectrum amplitude and phase ratios, respectively.

## 6. Acknowledgement

The research was conducted as part of the research on “building soundness evaluation based on earthquake observation and vibration monitoring (FY 2016-2018)”, which is a work group for young scientists in the Tsukuba building research institute council (BRIC). ViewWave (Ver2.2.2) was used to draw some figures and perform part of the analysis. We acknowledge Mr. Ohara and Mr. Jinno (Sonas, Inc.) for providing some measurement devices.

## 7. References

[1] Nakamura M., Yasui Y. (1999): Damage evaluation of a steel structure subjected to strong earthquake motion based on ambient vibration measurements, J. Str. Eng., AIJ, 515, 61-68, doi:10.3130/aijs.64.61_1 (in Japanese with English abstract).



 

[2] Kurata N. (2016): A reports on the monitoring for architectural buildings and infrastructure as society, J. Soc. Instr. Contr. Eng., SICE, 55 (3), 197-202 (in Japanese).

[3] Yamamoto S. (1999): Health-monitoring, Kyoritsu Shuppan, 255p (in Japanese).

[4] Nakamura M., En K., Ishikawa R., Miura K. (2014): Technology for instantaneous estimation of structural damage, Obayashi corp. TRI, 78 (in Japanese).

[5] Saito D. (2015): A system for the decision of structural soundness "Yuremoni", J. Tech. NTT, 48-49 (in Japanese).

[6] Nakamura M. (2016): Similarity and differences between strong motion observation and structural monitoring, PD on annual meeting of AIJ, 4-12 (in Japanese).

[7] Kinoshita S. (1998): Kyoshin net (K-NET), Bull. Seism. Soc. Am., Vol.69, No.4, 309-332.

[8] Aoi S., Kunugi T., Fujiwara H. (2004): Strong-motion seismograph network operated by NIED: K-NET and KiK-net, J. Japan Assoc. Earth. Eng., 4 (3), 65-74.

[9] Ministry of Internal Affairs and Communications (2017): Annual report on information and communication, http://www.soumu.go.jp/johotsusintokei/whitepaper/ja/h29/pdf/n1100000.pdf (accessed 2018-08-09; in Japanese).

[10] Qingkai K., Allen M. R., Kohler D. M., Heaton H. T., Bunn J. (2018): Structural Health Monitoring of Buildings Using Smartphone Sensors, SRL, 594–602.

[11] Naito S. (2015): A study on the construction of network using seismometers located high density with cloud server, Nagoya University, http://www.gensai.nagoya-u.ac.jp/nankai-t/download/nied/6_nied_naito.pdf (accessed 2018-08-09; in Japanese)

[12] Tsuchimoto K. (2016): Evaluation to the workability on the construction of CLT and 6-story wood framework wall system, BRI (in Japanese).

[13] Kunugi T., AOI S., Fujiwara H. (2009): Strong-Motion Observation in Japan -History and Perspective-, J. Seism. Soc. Japan. 2nd ser., 61, 19-34, doi:10.4294/zisin.61.19 (in Japanese with English abstract).

[14] Takahashi R. (1957): "SMAC" Strong Motion Accelerometer, J. Seism. Soc. Japan. 2nd ser., 6 (3), 117-231, doi:10.4294/zisin1948.6.3_117 (in Japanese with English abstract).

[15] Kashima T. (2017): A report on the strong motion observation with 60 years, BRI.

[16] JABS (2017): Lessons from Kumamoto Earthquake, AIJ, 132 (1697), 4-33 (in Japanese).

[17] Tokyo metropolitan (2012): Ordinance for persons difficult to return by Tokyo metropolitan, https://www.bousai.metro.tokyo.lg.jp/kitaku_portal/1000050/1000536.html (in Japanese).

[18] Shiraishi M., Morii T., Okada K., Sugimoto K., Sato T., Kurata M., Tobita J. (2017): Local damage detection using densely deployed vibration sensors and output error of substructures -System verification in large shaking table test of steel high-rise building-, J. Str. Eng., AIJ, 82 (736), 801-811, doi:10.3130/aijs.82.801 (in Japanese with English abstract).

[19] Kashima T. (2016): Development of strong motion observation in soil-building system, PD on annual meeting of AIJ, 16-23 (in Japanese).

[20] Suzuki M., Nagayama T., Ohara S., Morikawa H. (2017): Structural Monitoring Using Concurrent Transmission Flooding, IEICE Trans. Comm., J100–B (12), 952-960, doi:10.14923/transcomj.2017ASI0002 (in Japanese).

[21] Masuda Y. (2014): Development of building continuity support system as building management system for business continuity -Fundamental research on implementation of resilient buildings-, J. Env. Eng., AIJ, 79 (700), 535-544, doi:10.3130/aije.79.535 (in Japanese with English abstract).

[22] Kashima T. (2002): A system for observation to applicable for nationwide use, 3th sym. SMO, AIJ, 21-24 (in Japanese).

[23] Miura A., Nakano K., Sakai S. (2018): An examination based on the shaking table test for investigating the performance of MEMS-sensor installed in smart devices, Annual meeting, AIJ, 209-210 (in Japanese).



 

[24] Watabe T., Tezuka J., Watakabe M., Inai S., Nakamura T., Ishida T. (2012): Structural Vibration Tests using AMD Installed Full-Scale Building Part 1. Summary of the structural design and Simulation Analysis, Annual meeting, AIJ, 1079-1080 (in Japanese).

[25] Narita N., Yasui M., Yamamoto T., Kosaka H. (2017): The method to verify the performance of response in frequency domain with inexpensive MEMS accelerometers, Annual meeting, JAEE (in Japanese).

[26] Kosaka H., Kashima T. (2018): Verification of amplitude and phase characteristics of inexpensive MEMS accelerometers, Annual meeting, AIJ, 211-212 (in Japanese).

[27] Kashima T., Fukuba T., Nakagawa H. (2017): Strong motion instrumentation in a 6-story wooden experimental building and analysis of its dynamic characteristics, Annual meeting, AIJ, 505-506 (in Japanese).



 